Measurement of activation cross sections with d-D neutrons in the energy range of 2.0-3.2 MeV

Toshiaki Shimizu[1], Shinya Furuichi[1], Hitoshi Sakane[2], Michihiro Shibata[2], Kiyoshi Kawade[2], Yoshimi Kasugai[3], and Hiroshi Takeuchi[3]

[1] *Department of Nuclear Engineering, Nagoya University.*

[2] *Department of Energy Engineering and Science, Nagoya University.*

[3] *Japan Atomic Energy Research Institute*

e-mail: toshiaki_s@lycos.ne.jp

Activation cross sections for six (n,p) reactions were measured in the neutron energy range between 2.0 and 3.2 MeV. The measured target isotopes were ^{27}Al, ^{51}V, ^{61}Ni, ^{65}Cu, ^{69}Ga, and ^{92}Mo. The cross sections for ^{61}Ni, ^{69}Ga and ^{92}Mo were obtained at the first time. The cross sections are overestimated for ^{51}V, ^{69}Ga and ^{92}Mo in JENDL-3.2.

1 Introduction

Database of activation cross section for neutron energy up to 15 MeV was required for a design of fusion reactors. The cross section data are world-widely serviced as the evaluated libraries such as JENDL-3.2[1)] etc.. To evaluate the excitation function of cross section with accuracy, the experimental cross section data which covered with the neutron energy up to 15 MeV, are needed. Available cross section data in the neutron energy range between 13 and 15 MeV were reported. However, in the energy range between 2 and 13 MeV, the experimental data were rather scarce owing to the lack of available intense neutron source.

Using a KN3750 Van de Grraff accelerator at Nagoya University and a Fusion Neutronics Source (FNS) at Japan Atomic Energy Institute, we have measured (n,n'),(n,p) and (n,α) reaction cross sections in the energy range between 2.0 and 6.8 MeV [2),3)]. In previous works at FNS, the distance between the D-target and irradiation positions was chosen to be 10 cm, a typical neutron fluence rate at irradiation positions was 5×10^6 n/cm^2·s. It is necessary for the measurement of much smaller cross section to irradiate the sample at more intense neutron field.

In the present work, the six (n,p) reaction cross sections have been measured in the energy range between 2.0 and 3.2 MeV by using an improved pneumatic transport system, which can obtain more than one order of magnitude larger than previous one.

2 Experiment

2.1 Irradiation and flux determination

The neutrons were generated by bombarding a deuterated titanium target on a copper backing with a d^+ beam of 1.5 mA and 350 keV using the Fusion Neutronics Source (FNS) at Japan Atomic Energy Research Institute. As shown in Fig.1, a pneumatic sample transport system is used to transport samples from the irradiation position to the measurement position rapidly. The system is composed six acrylic tubes of 0.1 mm in thickness. The angles of the irradiation positions with respect to the incident d^+ beam are between 0° and 155°, which covered the neutron energies ranging from 3.2 to 2.0 MeV.

In previous works, the samples were irradiated at the distance of 10 cm from the d-target. In the present arrangement, the samples were irradiated at 2 –6 cm. As shown in Fig. 2, the neutron fluence rate at irradiation positions were 5×10^6-10^8 n/cm^2/s, which was 20 times larger than a previous system. The neutron fluence rate were measured with use of the standard reaction ^{115}In(n,n')^{115m}In ($T_{1/2}$=4.486h), whose cross section data from JENDL Dosimetry File 99. The samples were sandwiched by two Indium foils of 10mm×10mm×0.2mm thick.

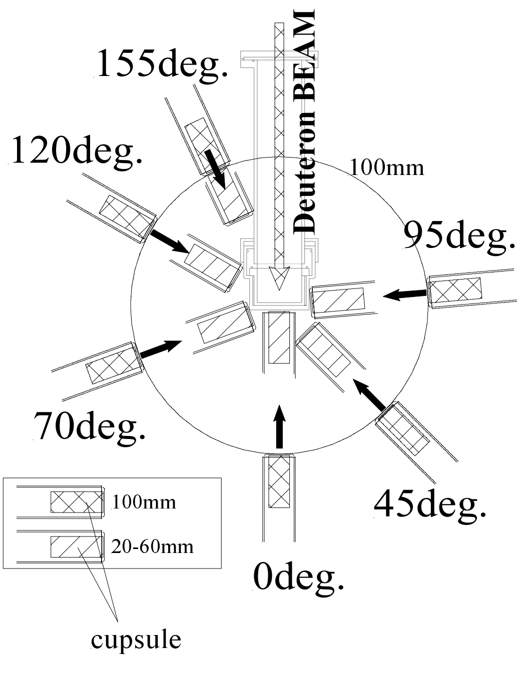

Fig.1: Schematic view of pneumatic transport system.

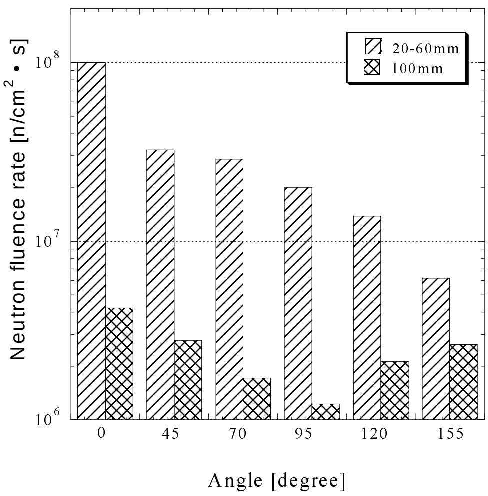

Fig.2: Typical neutron flux.

The energy spectrum of incident neutrons was determined by TOF measurement and the calculation from deuteron distribution in titanium target and neutron angular distribution as shown in Fig. 3. The effective neutron energies shift owing to angular distribution. As shown in Fig. 4, the effective energy of incident neutrons at each irradiation position was determined by the reaction-rate ratio of the ^{115}In(n,n')^{115m}In reaction to the ^{64}Zn(n,p)^{64}Cu reaction(JENDL-Dosimetry File). The measured effective neutron energies were well reproduced with the calculation value. The irradiation position is chosen to be 20 mm.

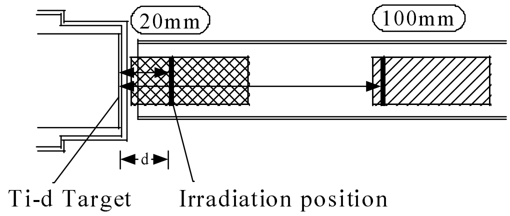

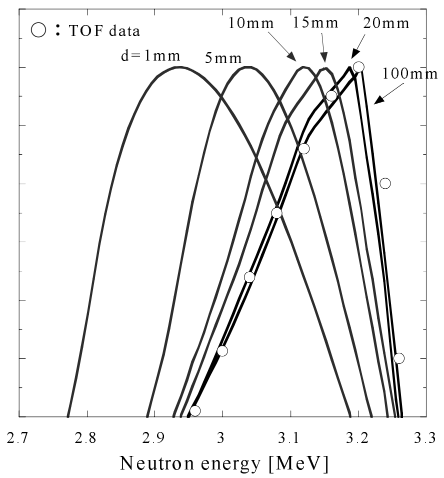

Fig.3 Neutron spectrum by TOF measurement and calculation at each irradiation position.

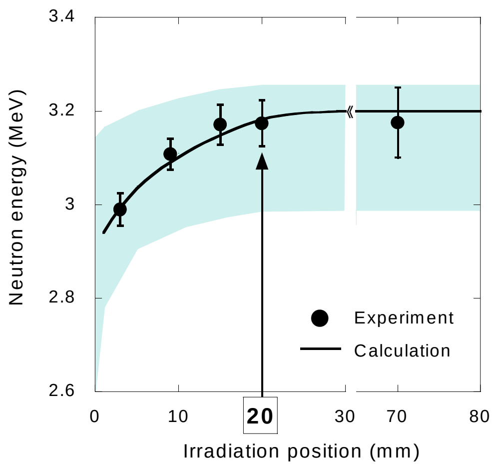

Fig.4 Neutron energy spread and effective energy at the distance between d-target and irradiation position.

Usually the target assembly at FNS 80° beam line was used as d-T and d-D neutron sources. Therefore, 14 MeV neutron was a little produced via T(d,n)^{4}He reaction owing to tritium contaminated in the extended tube. Since most cross sections at 14 MeV are 10^{2}-10^{3} times larger than that at 3 MeV, contribution of it was not ignored. We measured the d-T neutron fluence rate with use of the ^{93}Nb(n,2n)^{92m}Nb ($T_{1/2}$=10.15d, Q=-8.97MeV) reaction. The neutron fluence rate at each irradiation position was about 10^{-3} to d-D neutron.

2.2 Activity measurement

Gamma-ray emitted from the irradiated samples were measured with a well-type and a 30% closed end-type HPGe detectors. The efficiencies in the bottom of the well-type detector were 6-7 times larger than those at the close position of closed end-type detector. The closed end-type detector covered with a 5mm thick acrylic absorber in order to reduce beta rays, and the acrylic spacer with length at 4.5cm were also put on the detector. We call it standard position. The error in the efficiency at standard position is estimated to be 3%. The efficiency at the bottom of the well-type HPGe and at the surface of the end-cap of the coaxial-type HPGe were obtained by efficiency calibration method. To measure efficiently for weak induced activities, the irradiated samples were put on the surface of the acrylic plate at the distance of 5 mm from the end-cap of the HPGe detectors. The counts obtained at 5 mm were converted to those at 5 cm, using experimentally determined ratio of the efficiency at 5 mm to that of at 5 cm. This procedure improved the detection efficiency by a factor of about 7 in comparison with the measurements at 5 cm, and brought an additional error of only 1% to the results. The details of the procedure are described elsewhere (Sakane et al., 1999).

2.3 Decay data

In Table 1, measured reactions of associated decay data of the half-life, the gamma ray energy and the absolute intensity are listed together with Q-values.

Table 1: Measured reactions and decay parameters.

Reaction	Half life	Eγ (keV)	Iγ (%)	Q-value (keV)
$^{27}Al(n,p)^{27}Mg$	9.458min	843.74	71.8(8)	-1827.99
$^{51}V(n,p)^{51}Ti$	5.76min	320.0842	93.1(4)	-1688.30
$^{61}Ni(n,p)^{61}Co$	1.65h	67.412	84.7(4)	-539.38
$^{65}Cu(n,p)^{65}Ni$	2.52h	1481.84	23.59(14)	-1354.79
$^{69}Ga(n,p)^{69m}Zn$	13.76h	438.63	94.8(2)	-123.64
$^{92}Mo(n,p)^{92m}Nb$	10.15d	934.46	99.07(4)	425.84

2.4 Corrections

The following principal corrections were made for deduction of the cross sections. The details of procedures are described elsewhere (Kawade et al., submitted to Nucl. Instr. Meth.). Corrections were made for time fluctuation of neutron flux, thickness of samples, self absorption of γ-ray, summing effect of γ-ray and contribution of low energy neutron and d-T neutrons.

3 Results and discussion

The numerical values of the cross sections measured in the present study are given in Table 2. The present cross section data are shown in Fig. 5 together with the previous data[4)-6)] and the evaluated data in JENDL-3.2, -Activation File and -Dosimetry File.

The cross section data of six (n,p) reactions were obtained in the energy range between 2.0 and 3.2 MeV. The cross sections for ^{61}Ni, ^{69}Ga and ^{92}Mo were obtained at the first time. The cross sections are overestimated for ^{51}V, ^{69}Ga and ^{92}Mo in JENDL-3.2.

4 Conclusion

We have measured the cross sections down to about 10 micro barn for short-lived nuclei using the improved pneumatic sample transport system and a high efficient well-Type HPGe detector.

References

(1) T.Nakagawa, et al., Japanese Evaluated Nuclear Data Library Varsion 3 Revision-2: JENDL-3.2. Nucl. Sci. Technol., 32, 1259 (1995).
(2) T. Furuta et al., JAERI-Conf 99-002, 186 (1999).
(3) T. Senga et al., JAERI-Conf 2000-005, 208 (2000).
(4) Hussain et al., App. Radiat. Isotopes, 34, (4), 731 (1983).
(5) Smith et al., Ann. Nucl. Energy, 11, 623 (1984).
(6) D.C.Santry et al., Can. Jour. Phys., 44, 1183 (1965).

Table 2: Measured cross section data.

Reaction	Abundance (%)	En (MeV)			
		3.2	3.0	2.7	2.5
^{27}Al(n,p)^{27}Mg	100 (natural)	1.58(8)	0.58(6)	0.08(4)	-
^{51}V(n,p)^{51}Ti	99.75 (natural)	0.029(7)	0.014(8)	-	-
^{61}Ni(n,p)^{61}Co	88.84 (enriched)	1.3(1)	0.65(11)	-	0.20(8)
^{65}Cu(n,p)^{65}Ni	99.61 (enriched)	0.09(2)	0.04(2)	-	-
^{69}Ga(n,p)^{69m}Zn	60.108 (natural)	0.59(7)	0.33(6)	0.20(3)	0.13(3)
^{92}Mo(n,p)^{92m}Nb	97.37 (enriched)	3.1(2)	2.0(2)	1.6(3)	1.0(3)

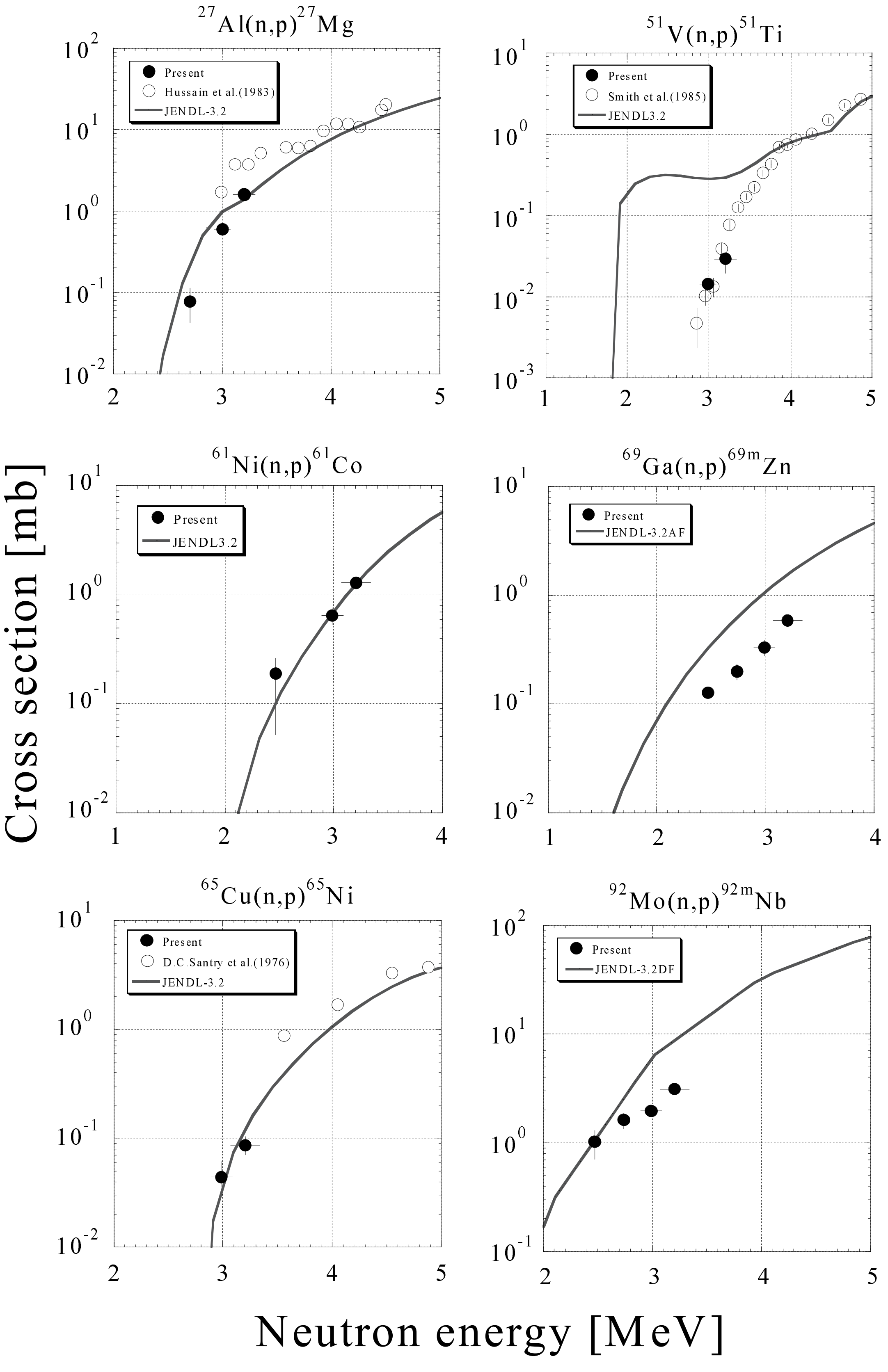

Fig. 5 Cross section data for the (n,p) reactions.